

Concise Explanations of Neural Networks using Adversarial Training

Prasad Chalasani¹ Jiefeng Chen² Somesh Jha^{1,2} Xi Wu³

Abstract

We show new connections between adversarial learning and explainability in Deep Neural Networks (DNNs). One form of explanation of the output of a neural network model in terms of its input features, is a vector of feature-attributions using the Integrated Gradient (IG) method. Two desirable characteristics of an attribution-based explanation are: (1) *sparseness*: the attributions of irrelevant or weakly relevant features should be negligible, thus resulting in *concise* explanations in terms of the significant features, and (2) *stability*: it should not vary significantly within a small local neighborhood of the input.

Our first contribution is a theoretical exploration of these connections for a class of 1-layer networks (which includes models such as logistic regression), for which we show that (a) adversarial training using an ℓ_∞ -bounded adversary produces models with sparse IG vectors, and (b) natural model-training while encouraging stable IG-explanations (via an extra term in the loss function), is equivalent to adversarial training. Our second contribution is an empirical verification of phenomenon (a), which we show, somewhat surprisingly, occurs *not only in 1-layer networks, but also DNNs trained on standard image datasets*: adversarial training with ℓ_∞ -bounded perturbations, yields significantly sparser IG vectors, with little degradation in performance on natural test data, compared to natural training. Moreover, the sparseness of the IG vectors is significantly better than that achievable via ℓ_1 -regularized natural training.

1. Introduction

Despite the recent dramatic success of deep learning models in a variety of domains, two concerns have surfaced about these models:

¹XaiPient ²University of Wisconsin at Madison ³Google. Correspondence to: Prasad Chalasani <pchalasani@gmail.com>.

Vulnerability to Adversarial Attacks: We can abstractly think of a neural network model as a function $F(\mathbf{x})$ of a d -dimensional input vector $\mathbf{x} \in \mathbb{R}^d$, and the range of F is either a discrete set of class-labels, or a continuous value such as a probability. Many of these models can be foiled by an adversary who imperceptibly (to humans) alters the input \mathbf{x} by adding a perturbation $\delta \in \mathbb{R}^d$ so that $F(\mathbf{x} + \delta)$ is very different from $F(\mathbf{x})$ (Szegedy et al., 2013; Goodfellow et al., 2014; Papernot et al., 2015; Biggio et al., 2013). *Adversarial training* (or *adversarial learning*) has recently been proposed as a method for training models that are robust to such attacks, by applying techniques from the area of Robust Optimization (Madry et al., 2017; Sinha et al., 2018). The core idea of adversarial training is simple: we define a set S of allowed perturbations $\delta \in \mathbb{R}^d$ that we want to "robustify" against (e.g. S could be the set of δ where $\|\delta\|_\infty \leq \varepsilon$), and perform model-training using Stochastic Gradient Descent exactly as in natural training, except that each training example x is perturbed adversarially, i.e. replaced by $x + \delta^*$ where $\delta^* \in S$ maximizes the example's loss-contribution.

Explainability: One way to address the well-known lack of explainability of deep learning models is *feature attribution*, which aims to explain the output of a model $F(\mathbf{x})$ as a vector $A_F(\mathbf{x})$ of the contributions from the *features* \mathbf{x} . A particularly noteworthy feature-attribution technique is the *Integrated Gradients* (IG) method (Sundararajan et al., 2017), which has a number of intuitively appealing axiomatic properties. Thus the IG-vector $IG_F(\mathbf{x})$ can be viewed as an explanation for $F(\mathbf{x})$. For such an explanation to be human-friendly, it is highly desirable (Molnar, 2019) that the IG-vector is *sparse*, i.e., only the features that are truly predictive of the output $F(\mathbf{x})$ should have significant contributions, and irrelevant or weakly-relevant features should have negligible contributions. A sparse attribution makes it possible to produce a *concise* explanation, where only the input features with significant contributions are included. For instance if the model F is used for a loan approval decision, then various stakeholders (e.g., customers, data-scientists and regulators) would like to know the reason for a specific decision in simple terms. In practice however, due to artifacts in the training data or process, the IG vector is often not sparse, and irrelevant or weakly-relevant features end up having significant contributions (Tan et al.,

2013). Another desirable property of a good explanation is *stability*: the IG-vector should not vary significantly within a small local neighborhood of the input x . Similar to the lack of concise explainability, natural training often results in explanations that lack stability (Alvarez-Melis & Jaakkola, 2018).

This paper shows new connections between adversarial robustness and the above-mentioned aspects of explainability, namely conciseness and stability of explanations.

Our first set of results show via a *theoretical* analysis that $\ell_\infty(\varepsilon)$ -adversarial training of 1-layer networks tends to produce sparse IG vectors (which in turn leads to concise explanations). In particular, under some assumptions, we show (Theorem 3.1) that for a general class of convex loss functions (which includes popular loss functions used in 1-layer networks, such as logistic and hinge loss), and adversarial perturbations δ satisfying $\|\delta\|_\infty \leq \varepsilon$, the weights of "weak" features are on average more aggressively shrunk toward zero than during natural training, and the rate of shrinkage is proportional to the amount by which ε exceeds a certain measure of the "strength" of the feature. This shows that $\ell_\infty(\varepsilon)$ -adversarial training tends to produce sparse *weight vectors* in popular 1-layer models. In Sec. 4 we show (Lemma 4.1) a closed form formula for the IG vector of 1-layer models, that makes it clear that in these models, sparseness of the *weight vector* directly implies sparseness of the *IG vector*.

In Section 6 we *empirically* demonstrate that this "IG Sparsification" effect of $\ell_\infty(\varepsilon)$ -adversarial training holds not only for 1-layer networks (e.g. logistic regression models), but also for Deep Convolutional Networks used for image classification. Specifically, we show this phenomenon via experiments applying $\ell_\infty(\varepsilon)$ -adversarial training to (a) Convolutional Neural Networks on public benchmark image datasets MNIST (LeCun & Cortes, 2010) and Fashion-MNIST (Xiao et al., 2017), and (b) logistic regression models on the Mushroom and Spambase tabular datasets from the UCI Data Repository (Dheeru & Karra Taniskidou, 2017). In all of our experiments, we find that it is possible to choose an ℓ_∞ bound ε so that adversarial learning under this bound produces IG vectors that are sparse on average, *with little or no drop in performance on natural test data*. A visually striking example of this effect is shown in Fig. 1 (the Gini Index, introduced in Sec. 6, measures the sparseness of the map).

It is natural to wonder whether a traditional *weight-regularization* technique such as ℓ_1 -regularization can produce models with sparse IG vectors. In fact our experiments show that for logistic regression models, ℓ_1 -regularized training does yield IG vectors that are on average significantly sparser compared to IG vectors from natural (un-regularized) model-training, and the sparseness im-

provement is almost as good as that obtained with $\ell_\infty(\varepsilon)$ -adversarial training. This is not too surprising given our result (Lemma 4.1) that implies a direct link between sparseness of *weights* and sparseness of *IG vectors*, for 1-layer models. Intriguingly, this does not carry over to DNNs: for multi-layer models (such as the ConvNets we trained for the image datasets mentioned above) we find that with ℓ_1 -regularization, the IG sparseness improvement is significantly inferior to that obtainable from $\ell_\infty(\varepsilon)$ -adversarial training (when controlling for model accuracy on natural test data), as we show in Table 1, Fig. 2 and Fig. 3. Thus it appears that for DNNs, adversarial training confers properties that go beyond merely inducing sparseness of weights.

We also show theoretically (Sec. 5) that training 1-layer networks naturally, while encouraging stability of explanations (via a suitable term added to the loss function), is in fact equivalent to adversarial training.

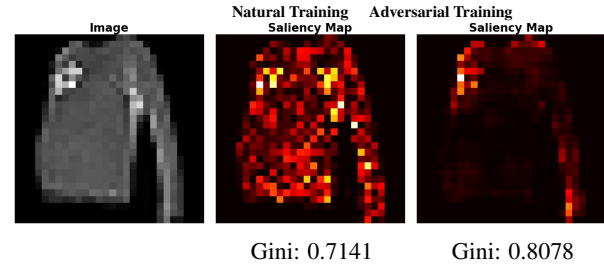


Figure 1: Both models correctly predict "Pullover", but the IG-based saliency map of the adversarially trained model is much sparser than that of the naturally trained model.

2. Setup and Assumptions

We assume there is a distribution \mathcal{D} of data points (\mathbf{x}, y) where $\mathbf{x} \in \mathbb{R}^d$ is an input feature vector, and $y \in \{\pm 1\}$ is its true label¹. For each $i \in [d]$, the i 'th component of \mathbf{x} represents an input feature, and is denoted by x_i . The model is assumed to have learnable parameters ("weights") $\mathbf{w} \in \mathbb{R}^d$, and for a given data point (\mathbf{x}, y) , the *loss* is given by some function $\mathcal{L}(\mathbf{x}, y; \mathbf{w})$. *Natural model training*² consists of minimizing the expected loss, known as *empirical risk*:

$$\mathbb{E}_{(\mathbf{x}, y) \sim \mathcal{D}}[\mathcal{L}(\mathbf{x}, y; \mathbf{w})]. \quad (1)$$

We sometimes assume the existence of an $\ell_\infty(\varepsilon)$ -adversary who may perturb the input example \mathbf{x} by adding a vector $\delta \in \mathbb{R}^d$ whose ℓ_∞ -norm is bounded by ε ; such a perturbation δ is referred to as an $\ell_\infty(\varepsilon)$ -perturbation. For a given data point (\mathbf{x}, y) and a given loss function $\mathcal{L}(\cdot)$, an $\ell_\infty(\varepsilon)$ -adversarial perturbation is a δ^* that maximizes the *adversarial loss* $\mathcal{L}(\mathbf{x} + \delta^*, y; \mathbf{w})$.

¹It is trivial to convert -1/1 labels to 0/1 labels and vice versa

²Also referred to as *standard training* by (Madry et al., 2017)

The aim of *adversarial training* (Madry et al., 2017) is to train a model that is *robust* to an $\ell_\infty(\varepsilon)$ -adversary (i.e. performs well in the presence of such an adversary), and consists of minimizing the expected $\ell_\infty(\varepsilon)$ -adversarial loss:

$$\mathbb{E}_{(\mathbf{x}, y) \sim \mathcal{D}} \left[\max_{\|\delta\|_\infty \leq \varepsilon} \mathcal{L}(\mathbf{x} + \delta, y; \mathbf{w}) \right]. \quad (2)$$

In the expectations (1) and (2) we often drop the subscript under \mathbb{E} when it is clear that the expectation is over $(\mathbf{x}, y) \sim \mathcal{D}$.

Some of our theoretical results make assumptions regarding the form and properties of the loss function \mathcal{L} , the properties of its first derivative, and the data distribution \mathcal{D} . For the sake of clarity, we highlight these assumptions (with mnemonic names) here for ease of future reference.

Assumption LOSS-INC *The loss function is of the form $\mathcal{L}(\mathbf{x}, y; \mathbf{w}) = g(-y\langle \mathbf{w}, \mathbf{x} \rangle)$ where g is a non-decreasing function.*

Assumption LOSS-CVX *The loss function is of the form $\mathcal{L}(\mathbf{x}, y; \mathbf{w}) = g(-y\langle \mathbf{w}, \mathbf{x} \rangle)$ where g is non-decreasing, almost-everywhere differentiable, and convex.*

Section B.1 in the Appendix shows that these Assumptions are satisfied by popular loss functions such as logistic and hinge loss. Incidentally, note that for any differentiable function g , g is convex if and only if its first-derivative g' is non-decreasing, and we will use this property in some of the proofs.

Assumption FEAT-INDEP *The features \mathbf{x} are conditionally independent given the label y , i.e. for any two distinct indices i, j , x_i is independent of x_j given y , or more compactly, $(x_i \perp x_j) \mid y$.*

This Assumption is used to prove Theorem 3.1 in the next Section, and is not as restrictive as it may first appear: one can imagine *clustering* features into groups that are conditionally independent of each other (given the label y), and extend our results to such clustered features; we leave this for future work.

Assumption FEAT-EXP *For each feature x_i , $i \in [d]$, $\mathbb{E}(x_i|y) = a_i y$ for some constant a_i .*

In Section B.2 (Appendix) we show that Assumption FEAT-EXP is without loss of generality, and it is worth observing that this Assumption implies

$$\mathbb{E}(yx_i) = \mathbb{E}[\mathbb{E}(yx_i|y)] = \mathbb{E}[y^2 a_i] = a_i. \quad (3)$$

$$\mathbb{E}(yx_i|y) = y\mathbb{E}[x_i|y] = y^2 a_i = a_i. \quad (4)$$

Note that for any j , the expectation $\mathbb{E}(yx_j)$ can be thought

of as representing the *degree of association*³ between feature x_j and label y . When the data distribution satisfies Assumption FEAT-EXP, $\mathbb{E}(yx_j) = a_j$, so we refer to a_j as the *directed strength*⁴ of feature x_j , and $|a_j|$ is referred to as the *absolute strength* of x_j . In particular when $|a_j|$ is large (small) we say that x_j is a *strong* (*weak*) feature.

3. Analysis of SGD Updates in Adversarial Training

One way to understand the characteristics of the weights in an adversarially-trained neural network model, is to analyze how the weights evolve during adversarial training under Stochastic Gradient Descent (SGD) optimization. One of the main results of this work is a theoretical characterization of the weight updates during a single SGD step, when applied to a randomly drawn data point $(\mathbf{x}, y) \sim \mathcal{D}$ that is subjected to an $\ell_\infty(\varepsilon)$ -adversarial perturbation.

Although the holy grail would be to do this for general DNNs (and we expect this will be quite difficult) we take a first step in this direction by analyzing *single-layer networks* with a single output (such as logistic regression models), where each weight is associated with an input feature. Intriguingly, our results (Theorem 3.1) show that for these models, $\ell_\infty(\varepsilon)$ -adversarial training tends to selectively reduce the weight-magnitude of *weakly relevant* or *irrelevant* features, and does so much more aggressively than natural training. In other words, natural training can result in models where many weak features have significant weights, whereas adversarial training would tend to push most of these weights close to zero. The resulting model weights would thus be more sparse, and the corresponding IG vectors would on average be more sparse as well (since in linear models, sparse weights imply sparse IG vectors; this is a consequence of Lemma 4.1) compared to naturally-trained models.

Our experiments (Sec. 6) show that indeed for logistic regression models (which satisfy the conditions of Theorem 3.1), adversarial training leads to sparse IG vectors. Surprisingly, our extensive experiments with Deep Convolutional Neural Networks on public image datasets demonstrate that this phenomenon extends to DNNs as well, even though our theoretical results only apply to 1-layer networks.

As a preliminary, it is easy to show the following expressions related to the $\ell_\infty(\varepsilon)$ -adversarial perturbation δ^* (See Lemmas 2 and 3 in Section C of the Appendix): For loss functions satisfying Assumption LOSS-INC, the $\ell_\infty(\varepsilon)$ -

³When the features are standardized to have mean 0, $\mathbb{E}(yx_j)$ is in fact the covariance of y and x_j .

⁴This is related to the feature "robustness" notion introduced in (Ilyas et al., 2019)

adversarial perturbation δ^* is given by:

$$\delta^* = -y \operatorname{sgn}(\mathbf{w})\varepsilon, \quad (5)$$

the corresponding $\ell_\infty(\varepsilon)$ -adversarial loss is

$$\mathcal{L}(\mathbf{x} + \delta^*, y; \mathbf{w}) = g(\varepsilon \|\mathbf{w}\|_1 - y \langle \mathbf{w}, \mathbf{x} \rangle), \quad (6)$$

and the gradient of this loss w.r.t. a weight w_i is

$$\begin{aligned} \frac{\partial \mathcal{L}(\mathbf{x} + \delta^*, y; \mathbf{w})}{\partial w_i} = \\ -g'(\varepsilon \|\mathbf{w}\|_1 - y \langle \mathbf{w}, \mathbf{x} \rangle) (yx_i - \operatorname{sgn}(w_i)\varepsilon). \end{aligned} \quad (7)$$

In our main result, the expectation of the g' term in (7) plays an important role, so we will use the following notation:

$$\overline{g'} := \mathbb{E}[g'(\varepsilon \|\mathbf{w}\|_1 - y \langle \mathbf{w}, \mathbf{x} \rangle)] \quad (8)$$

Ideally, we would like to understand the nature of the weight-vector \mathbf{w}^* that minimizes the expected adversarial loss (2). This is quite challenging, so rather than analyzing the *final* optimum of (2), we instead analyze how an SGD-based optimizer for (2) *updates* the model weights \mathbf{w} . We assume an idealized SGD process: (a) a data point (\mathbf{x}, y) is drawn from distribution \mathcal{D} , (b) \mathbf{x} is replaced by $\mathbf{x}' = \mathbf{x} + \delta^*$ where δ^* is an $\ell_\infty(\varepsilon)$ -adversarial perturbation with respect to the loss function \mathcal{L} , (c) each weight w_i is updated by an amount $\Delta w_i = -\partial \mathcal{L}(\mathbf{x}', y; \mathbf{w}) / \partial w_i$ (assuming a unit learning rate to avoid notational clutter). We are interested in the *expectation* of Δw_i , in order to understand what happens to a weight w_i *on average* during a single SGD step. In fact it will be useful to analyze the **expected SGD update** $\overline{\Delta w_i}$ defined as follows:

$$\overline{\Delta w_i} := \begin{cases} -\mathbb{E} \frac{\partial \mathcal{L}}{\partial w_i}, & \text{when } w_i = 0, \\ -\operatorname{sgn}(w_i) \mathbb{E} \frac{\partial \mathcal{L}}{\partial w_i}, & \text{when } w_i \neq 0, \end{cases} \quad (9)$$

When $w_i \neq 0$, a **positive (negative)** $\overline{\Delta w_i}$ indicates that during an SGD update on a randomly chosen data-point, on average the weight w_i **expands (shrinks)**, i.e. maintains its sign and increases (decreases) in absolute value.

The following result characterizes $\overline{\Delta w_i}$ (the proof is in Section D of the Appendix).

Theorem 3.1 (Expected SGD Update in Adversarial Training) *For any loss function \mathcal{L} satisfying Assumption LOSS-CVX and a data distribution \mathcal{D} satisfying Assumptions FEAT-INDEP and FEAT-EXP, if a data point (\mathbf{x}, y) is randomly drawn from \mathcal{D} , and \mathbf{x} is perturbed to $\mathbf{x}' = \mathbf{x} + \delta^*$, where δ^* is an $\ell_\infty(\varepsilon)$ -adversarial perturbation, then under the $\ell_\infty(\varepsilon)$ -adversarial loss $\mathcal{L}(\mathbf{x}', y; \mathbf{w})$, the expected SGD-update of weight w_i , namely $\overline{\Delta w_i}$, satisfies the following properties:*

1. If $w_i = 0$, then

$$\overline{\Delta w_i} = \overline{g'} a_i. \quad (10)$$

2. If $w_i \neq 0$, then

$$\overline{\Delta w_i} \leq \overline{g'} [a_i \operatorname{sgn}(w_i) - \varepsilon], \quad (11)$$

and equality holds in the limit as w_i approaches zero,

where $a_i = \mathbb{E}(x_i y)$ is the directed strength of feature x_i from Assumption FEAT-EXP, and $\overline{g'}$ is the expectation in (8).

For space reasons, a detailed discussion of the implications of this result is presented in Sec. D.2 of the Appendix. For the purposes of this paper, a key implication is that during SGD updates of $\ell_\infty(\varepsilon)$ -adversarially perturbed examples, the weights of features that are weakly correlated (or un-correlated) to the label tend to be aggressively pushed toward zero magnitude, and this aggressiveness is proportional to the difference between ε and the feature's label-correlation.

4. Feature Attribution using Integrated Gradients

Theorem 3.1 showed that $\ell_\infty(\varepsilon)$ -adversarial training tends to shrink the *weights* of features that are "weak" (relative to ε). We now show a link between weights and *explanations*, specifically explanations in the form of a vector of feature-attributions given by the *Integrated Gradients* (IG) method (Sundararajan et al., 2017), which is defined as follows: Suppose $F : \mathbb{R}^d \rightarrow \mathbb{R}$ is a real-valued function of an input vector. For example F could represent the output of a neural network, or even a loss function $\mathcal{L}(\mathbf{x}, y; \mathbf{w})$ when the label y and weights \mathbf{w} are held fixed. Let $\mathbf{x} \in \mathbb{R}^d$ be a specific input, and $\mathbf{u} \in \mathbb{R}^d$ be a baseline input. The IG is defined as the path integral of the gradients along the straight-line path from the baseline \mathbf{u} to the input \mathbf{x} . The IG along the i 'th dimension for an input \mathbf{x} and baseline \mathbf{u} is defined as:

$$\operatorname{IG}_i^F(\mathbf{x}, \mathbf{u}) := (x_i - u_i) \times \int_{\alpha=0}^1 \partial_i F(\mathbf{u} + \alpha(\mathbf{x} - \mathbf{u})) d\alpha, \quad (12)$$

where $\partial_i F(\mathbf{z})$ denotes the gradient of $F(\mathbf{v})$ along the i 'th dimension, at $\mathbf{v} = \mathbf{z}$. The vector of all IG components $\operatorname{IG}_i^F(\mathbf{x}, \mathbf{u})$ is denoted as $\operatorname{IG}^F(\mathbf{x}, \mathbf{u})$. Although we do not show \mathbf{w} explicitly as an argument in the notation $\operatorname{IG}^F(\mathbf{x}, \mathbf{u})$, it should be understood that the IG depends on the model weights \mathbf{w} since the function F depends on \mathbf{w} .

For general neural networks F , the authors of (Sundararajan et al., 2017) show that the IG attribution method satisfies a number of intuitively appealing properties that any reasonable attribution method should satisfy. They further show

how to approximate the IG integral (12) by a summation involving gradients at m equally-spaced points along the straight-line path from the baseline input \mathbf{u} to the actual input \mathbf{x} . While this approximation is reasonably efficient for a fixed example \mathbf{x} and dimension i , it can be prohibitively expensive for computing the IG values across a dataset of millions of examples and thousands of (sparse) features. A closed form expression for the IG would therefore be of significant interest, especially if the goal is to compute the IG over an entire dataset in order to glean aggregate feature importances. As we see below and in Section 5, such an expression also makes it easier to prove useful theoretical results.

The following Lemma (proved in Sec. E of the Appendix) shows a closed form exact expression for the $\text{IG}^F(\mathbf{x}, \mathbf{u})$ when $F(\mathbf{x})$ is of the form

$$F(\mathbf{x}) = A(\langle \mathbf{w}, \mathbf{x} \rangle), \quad (13)$$

where $\mathbf{w} \in \mathbb{R}^d$ is a vector of weights, A is a differentiable scalar-valued function, and $\langle \mathbf{w}, \mathbf{x} \rangle$ denotes the dot product of \mathbf{w} and \mathbf{x} . Note that this form of F could represent a single-layer neural network with any differentiable activation function (e.g., logistic (sigmoid) activation $A(\mathbf{z}) = 1/[1 + \exp(-\mathbf{z})]$ or Poisson activation $A(\mathbf{z}) = \exp(\mathbf{z})$), or a differentiable loss function, such as those that satisfy Assumption LOSS-INC for a fixed label y and weight-vector \mathbf{w} . For brevity, we will refer to a function of the form (13) as representing a "1-Layer Network", with the understanding that it could equally well represent a suitable loss function.

Lemma 4.1 (IG Attribution for 1-layer Networks) *If $F(\mathbf{x})$ is computed by a 1-layer network (13) with weights vector \mathbf{w} , then the Integrated Gradients for all dimensions of \mathbf{x} relative to a baseline \mathbf{u} are given by:*

$$\text{IG}^F(\mathbf{x}, \mathbf{u}) = [F(\mathbf{x}) - F(\mathbf{u})] \frac{(\mathbf{x} - \mathbf{u}) \odot \mathbf{w}}{\langle \mathbf{x} - \mathbf{u}, \mathbf{w} \rangle}, \quad (14)$$

where the \odot operator denotes the entry-wise product of vectors.

Thus for 1-layer networks, the IG of each feature is essentially proportional to the feature's fractional contribution to the logit-change $\langle \mathbf{x} - \mathbf{u}, \mathbf{w} \rangle$. This makes it clear that in such models, if the weight-vector \mathbf{w} is sparse, then the IG vector will also be correspondingly sparse. Recall that theorem 3.1 suggests that $\ell_\infty(\varepsilon)$ -adversarial training tends to shrink the weights of "weak" features. This is in fact what we see in the experimental results (Section 6): real-world tabular datasets often tend to have several such weak features, and $\ell_\infty(\varepsilon)$ -adversarial training (with a suitably chosen ε) of logistic regression models results in a sparse weight-vector, and hence a sparse IG vector as well. This also explains

why natural training with ℓ_1 regularization is able to produce models where on average the sparseness of IG vectors is close to the sparseness resulting from adversarial training. On the other hand, for Deep Neural Networks, there is no direct link between sparseness of weights and that of the IG vector, and in fact our experiments with DNNs on image datasets show that the IG vector sparseness resulting from $\ell_\infty(\varepsilon)$ -adversarial training is significantly better than that resulting from ℓ_1 -regularized natural training.

5. Training with Explanation Stability is equivalent to Adversarial Training

Suppose we use the IG method described in Sec. 4 as an explanation for the output of a model $F(\mathbf{x})$ on a specific input \mathbf{x} . A desirable property of an explainable model is that the explanation for the value of $F(\mathbf{x})$ is *stable* (Alvarez-Melis & Jaakkola, 2018), i.e., does not change much under small perturbations of the input \mathbf{x} . One way to formalize this is to say the following *worst-case* ℓ_1 -norm of the change in IG should be small:

$$\max_{\mathbf{x}' \in N(\mathbf{x}, \varepsilon)} \|\text{IG}^F(\mathbf{x}', \mathbf{u}) - \text{IG}^F(\mathbf{x}, \mathbf{u})\|_1, \quad (15)$$

where $N(\mathbf{x}, \varepsilon)$ denotes a suitable ε -neighborhood of \mathbf{x} , and \mathbf{u} is an appropriate baseline input vector. If the model F is a single-layer neural network, it would be a function of $\langle \mathbf{w}, \mathbf{x} \rangle$ for some weights \mathbf{w} , and typically when training such networks the loss is a function of $\langle \mathbf{w}, \mathbf{x} \rangle$ as well, so we would not change the essence of (15) much if instead of F in each IG, we use $\mathcal{L}(\mathbf{x}, y; \mathbf{w})$ for a fixed y ; let us denote this function by \mathcal{L}_y . Also intuitively, $\|\text{IG}^{\mathcal{L}_y}(\mathbf{x}', \mathbf{u}) - \text{IG}^{\mathcal{L}_y}(\mathbf{x}, \mathbf{u})\|_1$ is not too different from $\|\text{IG}^{\mathcal{L}_y}(\mathbf{x}', \mathbf{x})\|_1$. These observations motivate the following definition of *Stable-IG Empirical Risk*, which is a modification of the usual empirical risk (1), with a regularizer to encourage stable IG explanations:

$$\mathbb{E}_{(\mathbf{x}, y) \sim \mathcal{D}} \left[\mathcal{L}(\mathbf{x}, y; \mathbf{w}) + \max_{\|\mathbf{x}' - \mathbf{x}\|_\infty \leq \varepsilon} \|\text{IG}^{\mathcal{L}_y}(\mathbf{x}, \mathbf{x}')\|_1 \right]. \quad (16)$$

The following somewhat surprising result is proved in Section F of the Appendix.

Theorem 5.1 (Equivalence of Stable IG and Adversarial Robustness) *For loss functions $\mathcal{L}(\mathbf{x}, y; \mathbf{w})$ satisfying Assumption LOSS-CVX, the augmented loss inside the expectation (16) equals the $\ell_\infty(\varepsilon)$ -adversarial loss inside the expectation (2), i.e.*

$$\mathcal{L}(\mathbf{x}, y; \mathbf{w}) + \max_{\|\mathbf{x}' - \mathbf{x}\|_\infty \leq \varepsilon} \|\text{IG}^{\mathcal{L}_y}(\mathbf{x}, \mathbf{x}')\|_1 = \max_{\|\delta\|_\infty \leq \varepsilon} \mathcal{L}(\mathbf{x} + \delta, y; \mathbf{w}) \quad (17)$$

This implies that for loss functions satisfying Assumption **LOSS-CVX**, minimizing the Stable-IG Empirical Risk (16) is equivalent to minimizing the expected $\ell_\infty(\varepsilon)$ -adversarial loss. In other words, for this class of loss functions, *natural model training while encouraging IG stability is equivalent to $\ell_\infty(\varepsilon)$ -adversarial training!* Combined with Theorem 3.1 and the corresponding experimental results in Sec 6, this equivalence implies that, for this class of loss functions, and data distributions satisfying Assumption **FEAT-INDEP**, the explanations for the models produced by $\ell_\infty(\varepsilon)$ -adversarial training are both *concise* (due to the sparseness of the models), and *stable*.

6. Experiments

6.1. Hypotheses

Recall that one implication of Theorem 3.1 is the following: For 1-layer networks where the loss function satisfies Assumption **LOSS-CVX**, $\ell_\infty(\varepsilon)$ -adversarial training tends to more-aggressively prune the *weight-magnitudes* of "weak" features compared to natural training. In Sec. 4 we observed that a consequence of Lemma 4.1 is that for 1-layer models the sparseness of the weight vector implies sparseness of the IG vector. Thus a reasonable conjecture is that, for 1-layer networks, $\ell_\infty(\varepsilon)$ -adversarial training leads to models with sparse IG vectors.

What can we say about the *natural accuracy* (i.e. the accuracy on natural unperturbed test data) of such models? *In theory* it is possible (Tsipras et al., 2018) to construct a synthetic dataset where a model relies on a large number of weak features to achieve high natural accuracy, and $\ell_\infty(\varepsilon)$ -adversarial training would significantly reduce the contributions of these features, thus greatly lowering the natural accuracy of the resulting model. However we conjecture that this does not occur *in practice*, and pruning weak features as a result of $\ell_\infty(\varepsilon)$ -adversarial training does not significantly impact natural accuracy. Moreover, we conjecture that $\ell_\infty(\varepsilon)$ -adversarial training induces sparseness of the IG vectors in practical multi-layer Deep Neural Networks, not just 1-layer networks.

Thus the hypothesis we set out to verify experimentally is this: For several public datasets, it is possible to choose an $\varepsilon > 0$ such that $\ell_\infty(\varepsilon)$ -adversarial training of a suitable model (whether a single-layer or multi-layer neural network) results in models whose IG vectors (for test data points) are on average significantly sparser, and their natural accuracy is not much lower, compared to naturally trained models. We further hypothesize that the resulting sparseness of *IG vectors* is better than what can be achieved by a traditional *weight regularization* technique such as L1-regularization, for a comparable level of natural test accuracy.

6.2. Measuring Sparseness of an IG Vector

We quantify the sparseness of the IG vector $\text{IG}^F(\mathbf{x}, \mathbf{u})$ using the *Gini Index* applied to the absolute IG vector. For a vector \mathbf{v} of non-negative values, the Gini Index, denoted $G(\mathbf{v})$, is a metric for sparseness of \mathbf{v} that is known (Hurley & Rickard, 2009) to satisfy a number of desirable properties that are not simultaneously satisfied by other alternative measures. The measure was originally suggested by (Gini, 1936) to quantify income inequality in a population, and has also recently been used to quantify sparseness of weights in a neural network (Guest & Love, 2017). See Sec. H for a formal definition of the Gini Index. The Gini Index by definition lies in $[0,1]$, and a higher value indicates more sparseness.

Since the model F is clear from the context, and the baseline vector \mathbf{u} are fixed for a given dataset, we will denote the IG vector input \mathbf{x} simply as $\text{IG}(\mathbf{x})$, and our measure of sparseness is $G(|\text{IG}(\mathbf{x})|)$, which we denote for brevity as $\text{GIG}(\mathbf{x})$, and refer to informally as the *Gini of the IG*. As mentioned above, one of our hypotheses is that the IG vector sparseness produced by $\ell_\infty(\varepsilon)$ -adversarial training is much better than what can be achieved by natural training using ℓ_1 -regularization, for a comparable level of accuracy. To verify this hypothesis we will compare the sparseness of IG vectors resulting from three types of models: (a) N-model: *naturally-trained* model with no adversarial perturbations and no ℓ_1 -regularization, (b) A-model: $\ell_\infty(\varepsilon)$ -adversarially trained model, and (c) L-model: naturally trained model with ℓ_1 -regularization strength $\lambda > 0$. We denote the IG-sparseness resulting from these models respectively as $\text{GIG}^N(\mathbf{x})$, $\text{GIG}^A(\mathbf{x}; \varepsilon)$ and $\text{GIG}^L(\mathbf{x}; \lambda)$.

In several of our datasets, individual feature vectors are already quite sparse: for example in the MNIST dataset, most of the area consists of black pixels, and in the Mushroom dataset, after 1-hot encoding the 22 categorical features, the resulting 120-dimensional feature-vector is sparse. On such datasets, even an N-model can achieve a "good" level of sparseness of IGs in the absolute sense, i.e. $\text{GIG}^N(\mathbf{x})$ can be quite high. Therefore for all datasets we compare the *IG sparseness improvement* resulting from an A-model relative to an N-model, with that from an L-model relative to a N-model. Or more precisely, we will compare the two quantities defined below

$$\text{dGIG}^A(\mathbf{x}; \varepsilon) := \text{GIG}^A(\mathbf{x}; \varepsilon) - \text{GIG}^N(\mathbf{x}), \quad (18)$$

$$\text{dGIG}^L(\mathbf{x}; \lambda) := \text{GIG}^L(\mathbf{x}; \lambda) - \text{GIG}^N(\mathbf{x}). \quad (19)$$

The above quantities define the IG sparseness improvements for a *single* example \mathbf{x} . It will be convenient to define the overall sparseness improvement from a model, as measured on a test dataset, by averaging over all examples \mathbf{x} in that dataset. We denote the corresponding *average* sparseness metrics by $\text{GIG}^A(\varepsilon)$, $\text{GIG}^L(\lambda)$ and GIG^N . We then define

the *average sparseness improvement* of an A-model and L-model as:

$$dGIG^A(\varepsilon) := GIG^A(\varepsilon) - GIG^N, \quad (20)$$

$$dGIG^L(\lambda) := GIG^L(\lambda) - GIG^N. \quad (21)$$

We can thus re-state our hypotheses in terms of this notation: the average sparseness improvement $dGIG^A(\varepsilon)$ resulting from type-A models is high, and is significantly higher than the average sparseness improvement $dGIG^L(\lambda)$ resulting from type-L models.

6.3. Results

We ran experiments on four standard public benchmark datasets: two image datasets MNIST and Fashion-MNIST, and two tabular datasets from the UCI Data Repository: Mushroom and Spambase. Details of the datasets and training methodology are in Sec. 1.1 of the Appendix.

Table 1 shows a summary of some results on the above 4 datasets. Fig. 2 compares boxplots of the point-

Table 1: Results on 4 datasets. For each dataset, "A" indicates an $\ell_\infty(\varepsilon)$ -adversarially trained model with the indicated ε , and "L" indicates a naturally trained model with the indicated ℓ_1 -regularization strength λ . Column **dGIG** shows the average sparseness improvements of the models relative to the baseline naturally trained model, as measured by the $dGIG^A(\varepsilon)$ and $dGIG^L(\lambda)$ defined in Eqs. (20, 21). Column **AccDrop** indicates the drop in accuracy relative to the baseline model.

dataset	model	dGIG	AccDrop
MNIST	A ($\varepsilon = 0.3$)	0.06	0.8%
	L ($\lambda = 0.01$)	0.004	0.4%
Fashion-MNIST	A ($\varepsilon = 0.3$)	0.06	4.7%
	L ($\lambda = 0.01$)	0.008	3.4%
Mushroom	A ($\varepsilon = 0.1$)	0.07	1.5%
	L ($\lambda = 0.01$)	0.06	2.5%
Spambase	A ($\varepsilon = 0.1$)	0.12	0.9%
	L ($\lambda = 0.02$)	0.10	0.3%

wise sparseness-improvement metrics ($dGIG^A(\mathbf{x}; \varepsilon)$ and $dGIG^L(\mathbf{x}; \lambda)$) for each of the four datasets shown in Table 1. Fig. 3 shows for each dataset and model type (L and A), the Average Gini Index ($GIG^A(\varepsilon)$ and $GIG^L(\lambda)$) vs Accuracy achieved by choosing different values of ε or λ depending on the model type. These results make it clear that for comparable levels of accuracy, the sparseness of IG vectors from $\ell_\infty(\varepsilon)$ -adversarially trained models is much better than the sparseness from natural training with ℓ_1 -regularization. The effect is especially pronounced in

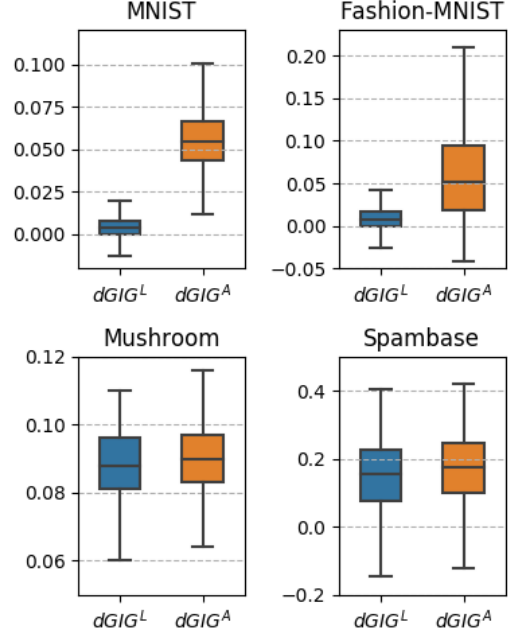


Figure 2: Boxplot of pointwise sparseness-improvements from adversarially trained models ($dGIG^A(\mathbf{x}, \varepsilon)$) and naturally trained models with ℓ_1 -regularization ($dGIG^L(\mathbf{x}, \lambda)$)

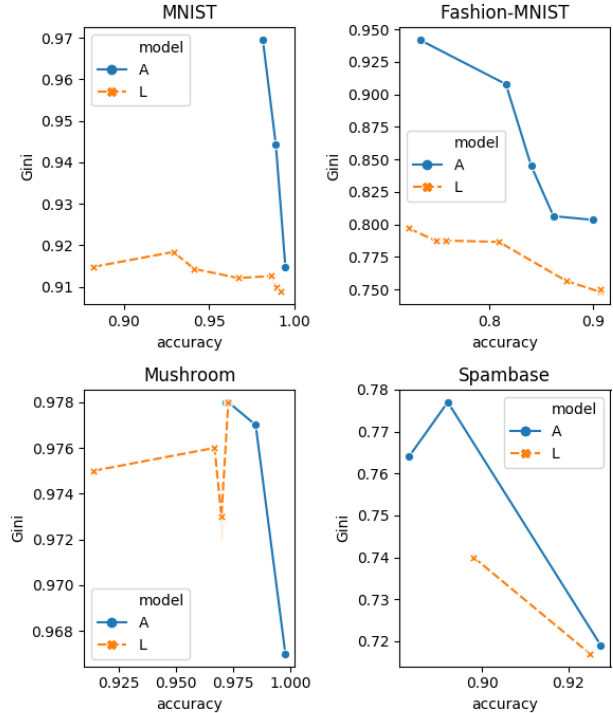


Figure 3: Average Gini Index of adversarially trained models ($GIG^A(\varepsilon)$, indicated by "A"), and that of naturally trained models ($GIG^L(\lambda)$, indicated by "L").

the two image datasets. The effect is less dramatic in the two tabular datasets, for which we train logistic regression models. As an explanation for why this is the case, we recall the discussion at the end of Sec. 4 where we derived a closed form expression for the IG of a 1-layer model: for such models, a sparse weight vector implies a sparse IG vector, and so it is not surprising that a *weight-regularization* technique such as ℓ_1 -regularization achieves IG sparseness close to that achieved by $\ell_\infty(\varepsilon)$ -adversarial training. The work of (Xu et al., 2009) is related to these observations: they explore the relationship between robust and regularized SVM classification, and show that in the case of SVMs, a robust classifier is equivalent to a regularized classifier. It is worth noting that even though IG sparseness produced by ℓ_1 -regularized logistic models (at least on the two tabular datasets) is close to that of $\ell_\infty(\varepsilon)$ -adversarial trained logistic models, the latter models confer additional benefits that the former do not: robustness to adversarial attacks, and stability of explanations (as we showed in Theorem 5.1).

For image classification models, *saliency maps* (Simonyan et al., 2014; Baehrens et al., 2010; Adebayo et al., 2018; Erhan et al., 2009) have recently emerged as a popular technique to visualize the contribution of an input pixel (as determined by an attribution method such as IG) to the classification of a model. We already gave an example of saliency maps in the Introduction (Fig. 1), and we show several more in Figs. I.6 and I.7 of the Appendix: for specific images, we compare the IG-based saliency maps of the N, A and L models; the brightness of a pixel is proportional to its IG value. In each case, all three models predicted the true class correctly and with high confidence. Once again it is evident that $\ell_\infty(\varepsilon)$ -adversarial training results in noticeably sparser IG-attributions, compared to natural training (with or without ℓ_1 -regularization).

7. Related Work

In contrast to the growing body of work on defenses against adversarial attacks (Yuan et al., 2017; Madry et al., 2017; Biggio et al., 2013) or explaining adversarial examples (Goodfellow et al., 2014; Tsipras et al., 2018), the focus of our paper is the connection between adversarial robustness and explainability. We view the process of adversarial training as a tool to produce more explainable models. A recent series of papers (Tsipras et al., 2018; Ilyas et al., 2019) essentially argues that adversarial examples exist because standard training produces models that are heavily reliant on highly predictive but *non-robust features* (which is similar to our notion of "weak" features in Sec 3) which are vulnerable to an adversary who can "flip" them and cause performance to degrade. Indeed the authors of (Ilyas et al., 2019) touch upon some connections between explainability and robustness, and conclude, "As such, producing human-

meaningful explanations that remain faithful to underlying models cannot be pursued independently from the training of the models themselves", by which they are implying that good explainability may require intervening in the model-training procedure itself; this is consistent with our findings. Another recent related paper (Kim et al., 2019) analyzes the effect of adversarial training on the interpretability of neural network loss gradients. We discuss other related work in the Appendix Section A.

8. Conclusion

We presented theoretical and experimental results that show a strong connection between adversarial robustness (under ℓ_∞ -bounded perturbations) and two desirable properties of model explanations: conciseness and stability. Specifically, we considered model explanations in the form of feature-attributions based on the Integrated Gradients (IG) methodology. For 1-layer models using a popular family of loss functions, we analyzed the expectation of weight-updates in an idealized Stochastic Gradient Descent (SGD) algorithm and showed that the weights of marginally relevant features tend to be aggressively pushed toward zero, thus producing sparse weights, and hence sparse IG vectors. For these models, we also theoretically showed that $\ell_\infty(\varepsilon)$ -adversarial training produces IG vectors that are stable to local perturbations. With extensive experiments, we demonstrated that the "IG sparsification" effect holds not only for 1-layer networks, but also for Deep Neural Networks trained on standard image benchmark datasets. Intriguingly, we found that the sparseness of IG vectors in naturally trained models with ℓ_1 -regularization, is significantly inferior to the IG sparseness achievable via $\ell_\infty(\varepsilon)$ -adversarial training. Our theoretical results are a first step in explaining some of these phenomena.

9. Acknowledgements

We are grateful to Aravind Sadagopan for running extensive experiments that appeared in an earlier version of the paper. We also thank Henry Prior for helpful comments on a draft, which significantly improved the presentation in the Introduction.

References

- Abramovich, F. and Grinshtein, V. High-dimensional classification by sparse logistic regression. June 2017. URL <http://arxiv.org/abs/1706.08344>.
- Adebayo, J., Gilmer, J., Muelly, M., Goodfellow, I., Hardt, M., and Kim, B. Sanity checks for saliency maps. In Bengio, S., Wallach, H., Larochelle, H., Grauman, K., Cesa-Bianchi, N., and Garnett, R. (eds.), *Advances in Neural Information Processing Systems 31*, pp. 9505–9515. Curran Associates, Inc., 2018. URL <http://papers.nips.cc/paper/8160-sanity-checks-for-saliency-maps.pdf>.
- Alvarez-Melis, D. and Jaakkola, T. S. On the robustness of interpretability methods. *arXiv preprint arXiv:1806.08049*, 2018. URL <http://arxiv.org/abs/1806.08049>.
- Baehrens, D., Schroeter, T., Harmeling, S., Kawanabe, M., Hansen, K., and Müller, K.-R. How to explain individual classification decisions. *J. Mach. Learn. Res.*, 11(Jun):1803–1831, 2010. URL <http://www.jmlr.org/papers/volume11/baehrens10a/baehrens10a.pdf>.
- Biggio, B., Corona, I., Maiorca, D., Nelson, B., Šrndić, N., Laskov, P., Giacinto, G., and Roli, F. Evasion attacks against machine learning at test time. In *Machine Learning and Knowledge Discovery in Databases*, pp. 387–402. Springer Berlin Heidelberg, 2013. URL http://dx.doi.org/10.1007/978-3-642-40994-3_25.
- Dheeru, D. and Karra Taniskidou, E. UCI machine learning repository, 2017. URL <http://archive.ics.uci.edu/ml>.
- Erhan, D., Bengio, Y., Courville, A., and Vincent, P. Visualizing higher-layer features of a deep network. *University of Montreal*, 2009. URL https://www.researchgate.net/profile/Aaron_Courville/publication/265022827_Visualizing_Higher-Layer_Features_of_a_Deep_Network/links/53ff82b00cf24c81027da530.pdf.
- Gini, C. On the measure of concentration with special reference to income and statistics. *Colorado College Publication, General Series*, 208:73–79, 1936.
- Goodfellow, I. J., Shlens, J., and Szegedy, C. Explaining and harnessing adversarial examples. December 2014. URL <http://arxiv.org/abs/1412.6572>.
- Guest, O. and Love, B. C. What the success of brain imaging implies about the neural code. *Elife*, 6, January 2017. URL <http://dx.doi.org/10.7554/eLife.21397>.
- Hurley, N. and Rickard, S. Comparing measures of sparsity. *IEEE Trans. Inf. Theory*, 55(10):4723–4741, October 2009. URL <http://dx.doi.org/10.1109/TIT.2009.2027527>.
- Ilyas, A., Santurkar, S., Tsipras, D., Engstrom, L., Tran, B., and Madry, A. Adversarial examples are not bugs, they are features. May 2019. URL <http://arxiv.org/abs/1905.02175>.
- Kim, B., Seo, J., and Jeon, T. Bridging adversarial robustness and gradient interpretability. *Safe Machine Learning workshop at ICLR*, 2019.
- LeCun, Y. and Cortes, C. MNIST handwritten digit database. 2010. URL <http://yann.lecun.com/exdb/mnist/>.
- Madry, A., Makelov, A., Schmidt, L., Tsipras, D., and Vladu, A. Towards deep learning models resistant to adversarial attacks. June 2017.
- Molnar, C. *Interpretable Machine Learning*. 2019. <https://christophm.github.io/interpretable-ml-book/>.
- Papernot, N., McDaniel, P., Jha, S., Fredrikson, M., Berkay Celik, Z., and Swami, A. The limitations of deep learning in adversarial settings. November 2015. URL <http://arxiv.org/abs/1511.07528>.
- Sankaranarayanan, S., Jain, A., Chellappa, R., and Lim, S. N. Regularizing deep networks using efficient layerwise adversarial training. May 2017. URL <http://arxiv.org/abs/1705.07819>.
- Shaham, U., Yamada, Y., and Negahban, S. Understanding adversarial training: Increasing local stability of neural nets through robust optimization. November 2015. URL <http://arxiv.org/abs/1511.05432>.
- Simonyan, K., Vedaldi, A., and Zisserman, A. Deep inside convolutional networks: Visualising image classification models and saliency maps. In *2nd International Conference on Learning Representations, ICLR 2014, Banff, AB, Canada, April 14-16, 2014, Workshop Track Proceedings*, 2014. URL <http://arxiv.org/abs/1312.6034>.
- Sinha, A., Namkoong, H., and Duchi, J. Certifying some distributional robustness with principled adversarial training. February 2018. URL <https://openreview.net/pdf?id=Hk6kPgZA->.

- Sundararajan, M., Taly, A., and Yan, Q. Axiomatic attribution for deep networks. March 2017.
- Szegedy, C., Zaremba, W., Sutskever, I., Bruna, J., Erhan, D., Goodfellow, I., and Fergus, R. Intriguing properties of neural networks. December 2013. URL <http://arxiv.org/abs/1312.6199>.
- Tan, M., Tsang, I. W., and Wang, L. Minimax sparse logistic regression for very high-dimensional feature selection. *IEEE Trans Neural Netw Learn Syst*, 24(10):1609–1622, October 2013. URL <http://dx.doi.org/10.1109/TNNLS.2013.2263427>.
- Tan, M., Tsang, I. W., and Wang, L. Towards ultrahigh dimensional feature selection for big data. *J. Mach. Learn. Res.*, 15(1):1371–1429, 2014. URL <http://www.jmlr.org/papers/volume15/tan14a/tan14a.pdf>.
- Tanay, T. and Griffin, L. D. A new angle on l2 regularization. *CoRR*, abs/1806.11186, 2018.
- Tsipras, D., Santurkar, S., Engstrom, L., Turner, A., and Madry, A. Robustness may be at odds with accuracy. May 2018. URL <http://arxiv.org/abs/1805.12152>.
- Xiao, H., Rasul, K., and Vollgraf, R. Fashion-MNIST: a novel image dataset for benchmarking machine learning algorithms. August 2017. URL <http://arxiv.org/abs/1708.07747>.
- Xu, H., Caramanis, C., and Mannor, S. Robustness and regularization of support vector machines. *J. Mach. Learn. Res.*, 10(Jul):1485–1510, 2009. URL <http://www.jmlr.org/papers/volume10/xu09b/xu09b.pdf>.
- Yuan, X., He, P., Zhu, Q., and Li, X. Adversarial examples: Attacks and defenses for deep learning. December 2017. URL <http://arxiv.org/abs/1712.07107>.

[Code for the experiments is available at <https://github.com/aiexplicability/advex>]

A. Additional Related Work

Section 7 discussed some of the work most directly related to this paper. Here we describe some additional related work.

Relation to work on Regularization Benefits of AML. There has been prior work on the *regularization benefits* of adversarial training (Xu et al., 2009; Szegedy et al., 2013; Goodfellow et al., 2014; Shaham et al., 2015; Sankaranarayanan et al., 2017; Tanay & Griffin, 2018), primarily in image-classification applications: when a model is adversarially trained, its classification accuracy on natural (i.e. un-perturbed) test data can improve. All of this prior work has focused on the *performance-improvement* (on natural test data) aspect of regularization, but none have examined the *feature-pruning* benefits explicitly. In contrast to this work, our primary interest is in the explainability benefits of adversarial training, and specifically the ability of adversarial training to significantly improve feature-concentration while maintaining (and often improving) performance on natural test data.

Adversarial Training vs Feature-Selection. Since our results show that adversarial training can effectively shrink the weights of irrelevant or weakly-relevant features (while preserving weights on relevant features), a legitimate counter-proposal might be that one could weed out such features beforehand via a pre-processing step where features with negligible label-correlations can be "removed" from the training process. Besides the fact that this scheme has no guarantees whatsoever with regard to adversarial robustness, there are some practical reasons why correlation-based feature selection is not as effective as adversarial training, in producing pruned models: (a) With adversarial training, one needs to simply try different values of the adversarial strength parameter ε and find a level where accuracy (or other metric such as AUC-ROC) is not impacted much but model-weights are significantly more concentrated; on the other hand with the correlation-based feature-pruning method, one needs to set up an iterative loop with gradually increasing correlation thresholds, and each time the input pre-processing pipeline needs to be re-executed with a reduced set of features. (b) When there are categorical features with large cardinalities, where just some of the categorical values have negligible feature-correlations, it is not even clear how one can "remove" these specific feature *values*, since the feature itself must still be used; at the very least it would require a re-encoding of the categorical feature each time a subset of its values is "dropped" (for example if a one-hot encoding or hashing scheme is used). Thus correlation-based feature-pruning is a much more cumbersome and inefficient process compared to adversarial training.

Adversarial Training vs Other Methods to Train Sparse Logistic Regression Models. (Tan et al., 2013; 2014) propose an approach to train sparse logistic regression models based on a min-max optimization problem that can be solved by the cutting plane algorithm. This requires a specially implemented custom optimization procedure. By contrast, $\ell_\infty(\varepsilon)$ -adversarial training can be implemented as a simple and efficient "bolt-on" layer on top of existing ML pipelines based on TensorFlow, PyTorch or SciKit-Learn, which makes it highly practical. Another paper (Abramovich & Grinshtein, 2017) proposes a feature selection procedure based on penalized maximum likelihood with a complexity penalty on the model size, but once again this requires special-purpose optimization code.

B. Discussion of Assumptions

B.1. Loss Functions Satisfying Assumption LOSS-CVX

We show here that several popular loss functions satisfy the Assumption LOSS-CVX.

Logistic NLL (Negative Log Likelihood) Loss.

$\mathcal{L}(\mathbf{x}, y; \mathbf{w}) = -\ln(\sigma(y\langle \mathbf{w}, \mathbf{x} \rangle)) = \ln(1 + \exp(-y\langle \mathbf{w}, \mathbf{x} \rangle))$, which can be written as $g(-y\langle \mathbf{w}, \mathbf{x} \rangle)$ where $g(z) = \ln(1 + e^z)$ is a non-decreasing and convex function.

Hinge Loss

$\mathcal{L}(\mathbf{x}, y; \mathbf{w}) = (1 - y\langle \mathbf{w}, \mathbf{x} \rangle)^+$, which can be written as $g(-y\langle \mathbf{w}, \mathbf{x} \rangle)$ where $g(z) = (1 + z)^+$ is non-decreasing and convex.

Softplus Hinge Loss.

$\mathcal{L}(\mathbf{x}, y; \mathbf{w}) = \ln(1 + \exp(1 - y\langle \mathbf{w}, \mathbf{x} \rangle))$, which can be written as $g(-y\langle \mathbf{w}, \mathbf{x} \rangle)$ where $g(z) = \ln(1 + e^{1+z})$, and clearly g is non-decreasing. Moreover the first derivative of g , $g'(z) = 1/(1 + e^{-1-z})$ is non-decreasing, and therefore g is convex.

B.2. Assumption FEAT-EXP is without loss of generality

While Assumption FEAT-EXP may seem restrictive, we show that there is in fact no loss of generality in making this assumption, when there are only two possible values of the label.

Lemma 1 (Form of conditional expectation of X given Y when $Y \in \{\pm 1\}$) *Given random variables X, Y where $Y \in \{\pm 1\}$, $\mathbb{E}(X|Y)$ must be of the form:*

$$\mathbb{E}(X|Y) = aY + c \quad (\text{B.22})$$

where

$$a = [\mathbb{E}(X|Y = 1) - \mathbb{E}(X|Y = -1)]/2 \quad (\text{B.23})$$

and

$$c = [\mathbb{E}(X|Y = 1) + \mathbb{E}(X|Y = -1)]/2 \quad (\text{B.24})$$

This implies that the random variable $X' = X - c$ satisfies $\mathbb{E}(X'|Y) = aY$.

Proof: Consider the function $f(Y) = \mathbb{E}(X|Y)$, and let $b_0 := f(-1)$ and $b_1 := f(1)$. Since there are only *two* values of Y that are of interest, we can represent $f(Y)$ by a *linear* function $aY + c$, and it is trivial to verify that $a = (b_1 - b_0)/2$ and $c = (b_1 + b_0)/2$ are the unique values that are consistent with $f(-1) = b_0$ and $f(1) = b_1$. \square

A consequence of this Lemma is that a dataset can be transformed into one satisfying Assumption FEAT-EXP by a simple translation of each x_i to a new feature

$$x'_i = x_i - 0.5 * [\mathbb{E}(x_i|y = 1) + \mathbb{E}(x_i|y = -1)]. \quad (\text{B.25})$$

C. Expressions for adversarial perturbation and loss-gradient

We show two simple preliminary results for loss functions that satisfy Assumption LOSS-INC: Lemma 2 shows a simple closed form expression for the $\ell_\infty(\varepsilon)$ -adversarial perturbation, and we use this result to derive an expression for the *gradient* of the $\ell_\infty(\varepsilon)$ -adversarial loss $\mathcal{L}(\mathbf{x} + \delta^*, y; \mathbf{w})$ with respect to a weight w_i (Lemma 3).

Lemma 2 (Closed form for $\ell_\infty(\varepsilon)$ -adversarial perturbation) *For a data point (\mathbf{x}, y) , given model weights \mathbf{w} , if the loss function $\mathcal{L}(\mathbf{x}, y; \mathbf{w})$ satisfies Assumption LOSS-INC, the $\ell_\infty(\varepsilon)$ -adversarial perturbation δ^* is given by:*

$$\delta^* = -y \operatorname{sgn}(\mathbf{w})\varepsilon, \quad (5)$$

and the corresponding $\ell_\infty(\varepsilon)$ -adversarial loss is

$$\mathcal{L}(\mathbf{x} + \delta^*, y; \mathbf{w}) = g(\varepsilon \|\mathbf{w}\|_1 - y\langle \mathbf{w}, \mathbf{x} \rangle) \quad (6)$$

Proof: Assumption LOSS-INC implies that the loss is non-increasing in $y\langle \mathbf{w}, \mathbf{x} \rangle$, and therefore the $\ell_\infty(\varepsilon)$ -perturbation δ^* of \mathbf{x} that maximizes the loss would be such that, for each $i \in [d]$, x_i is changed by an amount ε in the direction of $-y \operatorname{sgn}(w_i)$, and the result immediately follows. \square

Lemma 3 (Gradient of adversarial loss) *For any loss function satisfying Assumption LOSS-INC, for a given data point (\mathbf{x}, y) , the gradient of the $\ell_\infty(\varepsilon)$ -adversarial loss is given by:*

$$\frac{\partial \mathcal{L}(\mathbf{x} + \delta^*, y; \mathbf{w})}{\partial w_i} = -g'(\varepsilon \|\mathbf{w}\|_1 - y\langle \mathbf{w}, \mathbf{x} \rangle) (yx_i - \operatorname{sgn}(w_i)\varepsilon) \quad (7)$$

Proof: This is straightforward by substituting the expression (5) for δ^* in $g(-y\langle \mathbf{w}, \mathbf{x} + \delta^* \rangle)$, and applying the chain rule. \square

D. Expectation of SGD Weight Update

The following Lemma will be used to prove Theorem 3.1.

D.1. Upper bound on $\mathbb{E}[Zf(Z, V)]$

Lemma 4 (Upper Bound on expectation of $Zf(Z, V)$ when f is non-increasing in Z , $(Z \perp V)|Y$, and $\mathbb{E}(Z|Y) = \mathbb{E}(Z)$)
 For any random variables Z, V , if:

- $f(Z, V)$ is non-increasing in Z ,
- Z, V are conditionally independent given a third r.v. Y , and
- $\mathbb{E}(Z|Y) = \mathbb{E}(Z)$,

then

$$\mathbb{E}[Zf(Z, V)] \leq \mathbb{E}(Z)\mathbb{E}[f(Z, V)] \quad (\text{D.26})$$

Proof: Let $\bar{z} = \mathbb{E}(Z) = \mathbb{E}(Z|Y)$ and note that

$$\mathbb{E}[Zf(Z, V)] - \mathbb{E}[Z]\mathbb{E}[f(Z, V)] = \mathbb{E}[Zf(Z, V)] - \bar{z}\mathbb{E}[f(Z, V)] \quad (\text{D.27})$$

$$= \mathbb{E}[(Z - \bar{z})f(Z, V)] \quad (\text{D.28})$$

We want to now argue that $\mathbb{E}[(Z - \bar{z})f(\bar{z}, V)] = 0$. To see this, apply the Law of Total Expectation by conditioning on Y :

$$\begin{aligned} \mathbb{E}[(Z - \bar{z})f(\bar{z}, V)] &= \mathbb{E}\left[\mathbb{E}[(Z - \bar{z})f(\bar{z}, V)|Y]\right] \\ &= \mathbb{E}\left[\mathbb{E}[(Z - \bar{z})|Y]\mathbb{E}[f(\bar{z}, V)|Y]\right] \quad (\text{since } (Z \perp V)|Y) \end{aligned} \quad (\text{D.29})$$

$$= 0. \quad (\text{since } \mathbb{E}(Z|Y) = \mathbb{E}(Z) = \bar{z}) \quad (\text{D.30})$$

Since $\mathbb{E}[(Z - \bar{z})f(\bar{z}, V)] = 0$, we can subtract it from the last expectation in (D.28), and by linearity of expectations the RHS of (D.28) can be replaced by

$$\mathbb{E}[(Z - \bar{z})(f(Z, V) - f(\bar{z}, V))]. \quad (\text{D.31})$$

That fact that $f(Z, V)$ is non-increasing in Z implies that $(Z - \bar{z})(f(Z, V) - f(\bar{z}, V)) \leq 0$ for any value of Z and V , with equality when $Z = \bar{z}$. Therefore the expectation (D.31) is bounded above by zero, which implies the desired result. \square

Theorem 3.1 (Expected SGD Update in Adversarial Training) For any loss function \mathcal{L} satisfying Assumption *LOSS-CVX* and a data distribution \mathcal{D} satisfying Assumptions *FEAT-INDEP* and *FEAT-EXP*, if a data point (\mathbf{x}, y) is randomly drawn from \mathcal{D} , and \mathbf{x} is perturbed to $\mathbf{x}' = \mathbf{x} + \delta^*$, where δ^* is an $\ell_\infty(\varepsilon)$ -adversarial perturbation, then under the $\ell_\infty(\varepsilon)$ -adversarial loss $\mathcal{L}(\mathbf{x}', y; \mathbf{w})$, the expected SGD-update of weight w_i , namely $\overline{\Delta w_i}$, satisfies the following properties:

1. If $w_i = 0$, then

$$\overline{\Delta w_i} = \overline{g'} a_i. \quad (10)$$

2. If $w_i \neq 0$, then

$$\overline{\Delta w_i} \leq \overline{g'} [a_i \operatorname{sgn}(w_i) - \varepsilon], \quad (11)$$

and equality holds in the limit as w_i approaches zero,

where $a_i = \mathbb{E}(x_i y)$ is the directed strength of feature x_i from Assumption *FEAT-EXP*, and $\overline{g'}$ is the expectation in (8).

Proof: Consider the adversarial loss gradient expression (7) from Lemma 3. For the case $w_i = 0$, the negative expectation of the adversarial loss gradient is

$$\begin{aligned} \overline{\Delta w_i} &= \mathbb{E}[y x_i g'(\varepsilon) \|\mathbf{w}\|_1 - y \langle \mathbf{w}, \mathbf{x} \rangle] \\ &= \mathbb{E}\left[\mathbb{E}[y x_i g'(\varepsilon) \|\mathbf{w}\|_1 - y \langle \mathbf{w}, \mathbf{x} \rangle | y]\right] \\ &= \mathbb{E}\left[y \mathbb{E}[x_i g'(\varepsilon) \|\mathbf{w}\|_1 - y \langle \mathbf{w}, \mathbf{x} \rangle | y]\right], \end{aligned}$$

and in the last expectation above, we note that since $w_i = 0$ the argument of g' does not depend on x_i , and by Assumption **FEAT-INDEP** the features are conditionally independent given y , so the inner conditional expectation can be factored as a product of conditional expectations, which gives

$$\begin{aligned}\overline{\Delta w_i} &= \mathbb{E} \left[y \mathbb{E}(x_i | y) \mathbb{E} [g'(\varepsilon | \|\mathbf{w}\|_1 - y \langle \mathbf{w}, \mathbf{x} \rangle) | y] \right] \\ &= \mathbb{E} \left[y^2 a_i \mathbb{E} [g'(\varepsilon | \|\mathbf{w}\|_1 - y \langle \mathbf{w}, \mathbf{x} \rangle) | y] \right] && \text{(due to Assumption FEAT-EXP)} \\ &= a_i \mathbb{E} \left[\mathbb{E} [g'(\varepsilon | \|\mathbf{w}\|_1 - y \langle \mathbf{w}, \mathbf{x} \rangle) | y] \right] && \text{(since } y = \pm 1) \\ &= a_i \overline{g'},\end{aligned}\tag{D.32}$$

which establishes the first result.

Now consider the case $w_i \neq 0$. Starting with the adversarial loss gradient expression (7) from Lemma 3, multiplying throughout by $-\text{sgn}(w_i)$ and taking expectations results in

$$\overline{\Delta w_i} = \mathbb{E} \left[[yx_i \text{sgn}(w_i) - \varepsilon] g'(\varepsilon | \|\mathbf{w}\|_1 - y \langle \mathbf{w}, \mathbf{x} \rangle) \right]\tag{D.33}$$

where the expectation is with respect to a random choice of data-point (\mathbf{x}, y) . The argument of g' can be written as

$$\varepsilon | \|\mathbf{w}\|_1 - y \langle \mathbf{w}, \mathbf{x} \rangle = - \sum_{j=1}^d |w_j| (yx_j \text{sgn}(w_j) - \varepsilon).$$

For $j \in \{1, 2, \dots, d\}$ if we let Z_j denote the random variable corresponding to $yx_j \text{sgn}(w_j) - \varepsilon$, then the expectation (D.34) can be written as

$$\mathbb{E} \left[Z_i g' \left(- \sum_{j=1}^d |w_j| Z_j \right) \right] = \mathbb{E} [Z_i g'(V - |w_i| Z_i)],\tag{D.34}$$

where the random variable V denotes the negative sum of the $|w_j| Z_j$ terms over all j *except* $j = i$. Note that the last expectation above is with respect to the distribution of three random variables: Z_i , V , and the random variable Y corresponding to the label y of the data point. Since Z_i is a function of feature x_i and Y , and V is a function of the remaining features and Y , Assumption **FEAT-INDEP** (the features x_j are conditionally independent given the label Y) implies $(V \perp Z_i) | Y$. Moreover (3) and (4) imply that

$$\mathbb{E}(Z_i) = \mathbb{E}(Z_i | Y) = a_i \text{sgn}(w_i) - \varepsilon.\tag{D.35}$$

Since by Assumption **LOSS-CVX**, g' is a non-decreasing function, $g'(V - |w_i| Z_i)$ is *non-increasing* in Z_i . Thus all three conditions of Lemma 4 are satisfied, with the random variables Z, V, Y and function f in the Lemma corresponding to random variables Z_i, V, Y and function g' respectively in the present Theorem. It then follows from Lemma 4 that

$$\overline{\Delta w_i} \leq \mathbb{E}(Z_i) \overline{g'}\tag{D.36}$$

$$= \overline{g'} [a_i \text{sgn}(w_i) - \varepsilon],\tag{D.37}$$

which establishes the upper bound (11) for any $w_i \neq 0$. Now consider a $w_i \neq 0$ that is infinitesimally close to 0. In this case $\overline{\Delta w_i}$ equals the RHS of (D.34), and if we let $|w_i|$ approach zero,

$$\overline{\Delta w_i} = \mathbb{E}[Z_i g'(V)] = \mathbb{E}[\mathbb{E}[Z_i g'(V) | Y]] = \mathbb{E}[\mathbb{E}[Z_i | Y] \mathbb{E}[g'(V) | Y]],\tag{D.38}$$

where the last equality follows from the conditional independence of Z_i and V given Y . Using (D.35) the last expectation above simplifies to $(a_i \text{sgn}(w_i) - \varepsilon) \overline{g'}$, which establishes the equality result for non-zero infinitesimally small w_i . \square

D.2. Implications of Theorem 3.1

Note that $a_j \text{sgn}(w_j) > 0$ signifies that the sign of the weight w_j agrees with the *directed strength* a_j of feature x_j , and for brevity we simply say that *weight w_j is aligned*. Conversely when $a_j \text{sgn}(w_j) < 0$ we say that *weight w_j is mis-aligned*. With these observations in mind Theorem 3.1 implies the following:

Weights grow from zero in the correct direction. When $w_i = 0$, the expected SGD update $\overline{\Delta w_i}$ is proportional to the directed strength a_i of feature x_i , and if $\overline{g'} \neq 0$, this means that on average the SGD update causes the weight w_i to grow from zero in the *correct direction*. This is what one would expect from an SGD training procedure.

Mis-aligned weights w_i shrink at a rate proportional to $\varepsilon + |a_i|$. When $w_i \neq 0$, if w_i is *mis-aligned*, i.e. $a_i \operatorname{sgn}(w_i) < 0$, the upper bound in (11) is non-positive, and this means the expected SGD update is non-positive, and the weight w_i *shrinks* on average. Thus, mis-aligned weights shrink on average, at a rate proportional to the ℓ_∞ adversarial bound ε plus the absolute feature strength. In other words, all other factors remaining the same, adversarial training (i.e. with $\varepsilon > 0$) shrinks mis-aligned faster than natural training (i.e. with $\varepsilon = 0$).

If w_i is aligned, and $\varepsilon > |a_i|$ then it shrinks at a rate proportional to $\varepsilon - |a_i|$. What happens when a non-zero weight w_i is aligned, i.e. $a_i \operatorname{sgn}(w_i) > 0$? In this case if $\varepsilon > |a_i|$, then the upper-bound (11) on the expected SGD update is once again negative (assuming $\overline{g'} \neq 0$), which means adversarial training with a *sufficiently large* ε that dominates the absolute strength of a feature will cause the weight of that feature to shrink on average. This observation is key to explaining the "feature-pruning" behavior of adversarial training: "weak" features (relative to ε) are weeded out by the SGD updates.

If w_i is aligned, and $\varepsilon < |a_i|$, then w_i expands up to a certain point. If a non-zero weight w_i is aligned and $\varepsilon < |a_i|$, then the upper bound (11) on $\overline{\Delta w_i}$ is non-negative. Since the Theorem states that equality holds in the limit as w_i approaches zero, this means if $|w_i|$ is sufficiently small, the expected SGD update $\overline{\Delta w_i}$ is non-negative, i.e., the weight w_i expands on average. In other words, weights of aligned features expand on average up to a certain point, if ε does not dominate their strength.

Note that Assumption [LOSS-CVX](#) implies that $\overline{g'} \geq 0$, and when the model \mathbf{w} is "far" from the optimum, the values of $-y\langle \mathbf{w}, \mathbf{x} \rangle$ will tend to be large, and since g' is a non-decreasing function (Assumption [LOSS-CVX](#)), $\overline{g'}$ will be large as well. So we can interpret $\overline{g'}$ as being a proxy for "average model error". Thus during the initial iterations of SGD, this quantity will tend to be large and positive, and shrinks toward zero as the model approaches optimality. Since $\overline{g'}$ appears as a factor in (10) and (11), we can conclude that the above effects will be more pronounced in the initial stages of SGD and less so in the later stages. The experimental results described in Section 6 are consistent with several of the above effects.

E. Proof of Lemma 4.1

Lemma 4.1 (IG Attribution for 1-layer Networks) *If $F(\mathbf{x})$ is computed by a 1-layer network (13) with weights vector \mathbf{w} , then the Integrated Gradients for all dimensions of \mathbf{x} relative to a baseline \mathbf{u} are given by:*

$$\operatorname{IG}^F(\mathbf{x}, \mathbf{u}) = [F(\mathbf{x}) - F(\mathbf{u})] \frac{(\mathbf{x} - \mathbf{u}) \odot \mathbf{w}}{\langle \mathbf{x} - \mathbf{u}, \mathbf{w} \rangle}, \quad (14)$$

where the \odot operator denotes the entry-wise product of vectors.

Proof: Since the function F , the baseline input \mathbf{u} and weight vector \mathbf{w} are fixed, we omit them from $\operatorname{IG}^F(\mathbf{x}, \mathbf{u})$ and $\operatorname{IG}_i^F(\mathbf{x}, \mathbf{u})$ for brevity. Consider the partial derivative $\partial_i F(\mathbf{u} + \alpha(\mathbf{x} - \mathbf{u}))$ in the definition (12) of $\operatorname{IG}_i(\mathbf{x})$. For a given \mathbf{x}, \mathbf{u} and α , let \mathbf{v} denote the vector $\mathbf{u} + \alpha(\mathbf{x} - \mathbf{u})$. Then $\partial_i F(\mathbf{v}) = \partial F(\mathbf{v}) / \partial v_i$, and by applying the chain rule we get:

$$\partial_i F(\mathbf{v}) := \frac{\partial F(\mathbf{v})}{\partial v_i} = \frac{\partial A(\langle \mathbf{w}, \mathbf{v} \rangle)}{\partial v_i} = A'(z) \frac{\partial \langle \mathbf{w}, \mathbf{v} \rangle}{\partial v_i} = w_i A'(z),$$

where $A'(z)$ is the gradient of the activation A at $z = \langle \mathbf{w}, \mathbf{v} \rangle$. This implies that:

$$\begin{aligned} \frac{\partial F(\mathbf{v})}{\partial \alpha} &= \sum_{i=1}^d \left(\frac{\partial F(\mathbf{v})}{\partial v_i} \frac{\partial v_i}{\partial \alpha} \right) \\ &= \sum_{i=1}^d [w_i A'(z) (x_i - u_i)] \\ &= \langle \mathbf{x} - \mathbf{u}, \mathbf{w} \rangle A'(z) \end{aligned}$$

We can therefore write

$$dF(\mathbf{v}) = \langle \mathbf{x} - \mathbf{u}, \mathbf{w} \rangle A'(z) d\alpha,$$

and since $\langle \mathbf{x} - \mathbf{u}, \mathbf{w} \rangle$ is a scalar, this yields

$$A'(z)d\alpha = \frac{dF(\mathbf{v})}{\langle \mathbf{x} - \mathbf{u}, \mathbf{w} \rangle}$$

Using this equation the integral in the definition of $IG_i(\mathbf{x})$ can be written as

$$\begin{aligned} \int_{\alpha=0}^1 \partial_i F(\mathbf{v}) d\alpha &= \int_{\alpha=0}^1 w_i A'(z) d\alpha \\ &= \int_{\alpha=0}^1 w_i \frac{dF(\mathbf{v})}{\langle \mathbf{x} - \mathbf{u}, \mathbf{w} \rangle} \\ &= \frac{w_i}{\langle \mathbf{x} - \mathbf{u}, \mathbf{w} \rangle} \int_{\alpha=0}^1 dF(\mathbf{v}) \\ &= \frac{w_i}{\langle \mathbf{x} - \mathbf{u}, \mathbf{w} \rangle} [F(\mathbf{x}) - F(\mathbf{u})], \end{aligned} \tag{E.39}$$

where (E.39) follows from the fact that $(\mathbf{x} - \mathbf{u})$ and \mathbf{w} do not depend on α . Therefore from the definition (12) of $IG_i(\mathbf{x})$:

$$IG_i(\mathbf{x}) = [F(\mathbf{x}) - F(\mathbf{u})] \frac{(x_i - u_i)w_i}{\langle \mathbf{x} - \mathbf{u}, \mathbf{w} \rangle},$$

and this yields the expression (14) for $IG(\mathbf{x})$. \square

F. Proof of Theorem 5.1

Theorem 5.1 (Equivalence of Stable IG and Adversarial Robustness) For loss functions $\mathcal{L}(\mathbf{x}, y; \mathbf{w})$ satisfying Assumption **LOSS-CVX**, the augmented loss inside the expectation (16) equals the $\ell_\infty(\varepsilon)$ -adversarial loss inside the expectation (2), i.e.

$$\mathcal{L}(\mathbf{x}, y; \mathbf{w}) + \max_{\|\mathbf{x}' - \mathbf{x}\|_\infty \leq \varepsilon} \|IG^{\mathcal{L}_y}(\mathbf{x}, \mathbf{x}')\|_1 = \max_{\|\delta\|_\infty \leq \varepsilon} \mathcal{L}(\mathbf{x} + \delta, y; \mathbf{w}) \tag{F.40}$$

Proof: Recall that Assumption **LOSS-CVX** implies $\mathcal{L}(\mathbf{x}, y; \mathbf{w}) = g(-y\langle \mathbf{w}, \mathbf{x} \rangle)$ for some non-decreasing, differentiable, convex function g . Due to this special form of $\mathcal{L}(\mathbf{x}, y; \mathbf{w})$, the function \mathcal{L}_y is a differential function of $\langle \mathbf{w}, \mathbf{x} \rangle$, and by Lemma 4.1 the i 'th component of the IG term in (F.40) is

$$IG_i^{\mathcal{L}_y}(\mathbf{x}, \mathbf{x}'; \mathbf{w}) = \frac{w_i(\mathbf{x}' - \mathbf{x})_i}{\langle \mathbf{w}, \mathbf{x}' - \mathbf{x} \rangle} \cdot (g(-y\langle \mathbf{w}, \mathbf{x}' \rangle) - g(-y\langle \mathbf{w}, \mathbf{x} \rangle)),$$

and if we let $\Delta = \mathbf{x}' - \mathbf{x}$ (which satisfies that $\|\Delta\|_\infty \leq \varepsilon$), its absolute value can be written as

$$\frac{|g(-y\langle \mathbf{w}, \mathbf{x} \rangle - y\langle \mathbf{w}, \Delta \rangle) - g(-y\langle \mathbf{w}, \mathbf{x} \rangle)|}{|\langle \mathbf{w}, \Delta \rangle|} \cdot |w_i \Delta_i|$$

Let $z = -y\langle \mathbf{w}, \mathbf{x} \rangle$ and $\delta = -y\langle \mathbf{w}, \Delta \rangle$, this is further simplified as $\frac{|g(z+\delta) - g(z)|}{|\delta|} |w_i \Delta_i|$. By Assumption **LOSS-CVX**, g is convex, and therefore the "chord slope" $[g(z+\delta) - g(z)]/\delta$ cannot decrease as δ is increased. In particular to maximize the ℓ_1 -norm of the IG term in Eq (F.40), we can set δ to be largest possible value subject to the constraint $\|\Delta\|_\infty \leq \varepsilon$, and we achieve this by setting $\Delta_i = -y \operatorname{sgn}(w_i)\varepsilon$, for each dimension i . This yields $\delta = \|\mathbf{w}\|_1 \varepsilon$, and the second term on the LHS of (F.40) becomes

$$\begin{aligned} |g(z+\delta) - g(z)| \cdot \frac{\sum_i |w_i \Delta_i|}{|\delta|} &= |g(z + \varepsilon \|\mathbf{w}\|_1) - g(z)| \cdot \frac{\sum_i |w_i| \varepsilon}{\|\mathbf{w}\|_1 \varepsilon} \\ &= |g(z + \varepsilon \|\mathbf{w}\|_1) - g(z)| \\ &= g(z + \varepsilon \|\mathbf{w}\|_1) - g(z) \end{aligned}$$

where the last equality follows because g is nondecreasing. Since $\mathcal{L}(\mathbf{x}, y; \mathbf{w}) = g(z)$ by Assumption **LOSS-CVX**, the LHS of (F.40) simplifies to

$$g(-y\langle \mathbf{w}, \mathbf{x} \rangle + \varepsilon \|\mathbf{w}\|_1),$$

and by Eq. (5), this is exactly the $\ell_\infty(\varepsilon)$ -adversarial loss on the RHS of (F.40). \square

G. Aggregate IG Attribution over a Dataset

Recall that in Section 4 we defined $IG^F(\mathbf{x}, \mathbf{u})$ in Eq. (12) for a *single* input \mathbf{x} (relative to a baseline input \mathbf{u}). This gives us a sense of the "importance" of each input feature in explaining a *specific* model prediction $F(\mathbf{x})$. Now we describe some ways to produce *aggregate* importance metrics over an entire dataset. For brevity let us simply write $IG(\mathbf{x})$ and $IG_i(\mathbf{x})$ and omit F and \mathbf{u} since these are fixed for a given model and a given dataset.

Note that in Eq. 12, \mathbf{x} is assumed to be an input vector in "exploded" space, i.e., all categorical features are (explicitly or implicitly) one-hot encoded, and i is the position-index corresponding to either a specific numerical feature, or a categorical feature-value. Thus if i corresponds to a categorical feature-value, then for any input \mathbf{x} where $x_i = 0$ (i.e. the corresponding categorical feature-value is not "active" for that input), $IG_i(\mathbf{x}) = 0$. A natural definition of the overall importance of a feature (or feature-value) i for a given model F and dataset \mathcal{D} , is the average of $|IG_i(\mathbf{x})|$ over all inputs $\mathbf{x} \in \mathcal{D}$, which we refer to as the **Feature Value Impact** $FV_i[\mathcal{D}]$. For a categorical feature with m possible values, we can further define its **Feature-Impact** (FI) as the *sum* of $FV_i[\mathcal{D}]$ over all i corresponding to possible values of this categorical feature.

The FI metric is particularly useful in tabular datasets to gain an understanding of the aggregate importance of high-cardinality categorical features.

H. Definition of the Gini Index

The definition is adapted from (Hurley & Rickard, 2009): Suppose we are given a vector of non-negative values $\mathbf{v} = [v_1, v_2, v_3, \dots, v_d]$. The vector is first *sorted* in non-decreasing order, so that the resulting indices after sorting are $(1), (2), (3), \dots, (d)$, i.e., $v_{(k)}$ denotes the k 'th value in this sequence. Then the Gini Index is given by:

$$G(\mathbf{v}) = 1 - 2 \sum_{k=1}^d \frac{v_{(k)}}{\|\mathbf{v}\|_1} \left(\frac{d - k + 0.5}{d} \right). \quad (\text{H.41})$$

Another equivalent definition of the Gini Index is based on plotting the cumulative fractional contribution of the sorted values. In particular if the sorted non-negative values are $[v_{(1)}, v_{(2)}, \dots, v_{(d)}]$, and for $k \in [d]$, we plot k/d (the fraction of dimensions up to k) vs $\frac{\sum_{i=1}^k v_{(i)}}{\|\mathbf{v}\|_1}$ (the fraction of values until the k 'th dimension), then the Gini Index $G(\mathbf{v})$ is 0.5 minus the area under this curve

The Gini Index by definition lies in $[0,1]$, and a higher value indicates more sparseness. For example if just one of the $v_i > 0$ and all the rest are 0, then $G(\mathbf{v}) = 1.0$, indicating perfect sparseness. At the other extreme, if all v_i are equal to some positive constant, then $G(\mathbf{v}) = 0$.

I. Experiments

I.1. Experiment Datasets and Methodology

We experiment with 4 public benchmark datasets. Below we briefly describe each dataset and model-training details.

MNIST. This is a classic image benchmark dataset consisting of grayscale images of handwritten digits 0 to 9 in the form of 28 x 28 pixels, along with the correct class label (0 to 9) (LeCun & Cortes, 2010). We train a Deep Neural Network consisting of two convolutional layers with 32 and 64 filters respectively, each followed by 2x2 max-pooling, and a fully connected layer of size 1024. Note that this is identical to the state-of-the-art adversarially trained model used by (Madry et al., 2017). We use 50,000 images for training, and 10,000 images for testing. When computing the IG vector for an input image, we use the predicted probability of the *true class* as the function F in the definition (12) of IG. For training each of the model types on MNIST, we use the Adam optimizer with a learning rate 10^{-4} , with a batch size of 50. For the naturally-trained model (with or without ℓ_1 -regularization) we use 25,000 training steps. For adversarial training, we use 100,000 training steps overall, and to generate adversarial examples we use Projected Gradient Descent (PGD) with random start. The PGD hyperparameters depend on the specific ε bound on the ℓ_∞ -norm of the adversarial perturbations: the number of PGD steps was set as $\varepsilon * 100 + 10$, and the PGD step size was set to 0.01.

Fashion-MNIST. This is another image benchmark dataset which is a drop-in replacement for MNIST (Xiao et al., 2017). Images in this dataset depict wearables such as shirts and boots instead of digits. The image format, the number of classes, as well as the number of train/test examples are all identical to MNIST. We use the same model and training details as for

MNIST.

Mushroom. This is a standard tabular public dataset from the UCI Data Repository (Dheeru & Karra Taniskidou, 2017). The dataset consists of 8142 instances, each of which corresponds to a different mushroom species, and has 22 categorical features (and no numerical features), whose cardinalities are all under 10. The task is to classify an instance as edible (label=1) or not (label=0). We train a simple *logistic regression* model to predict the probability that the mushroom is edible, with a 70/30 train/test split, and use a 0.5 threshold to make the final classification. We train the models on 1-hot encoded feature vectors, and the IG computation is on these (sparse) 1-hot vectors, with the output function F being the final predicted probability. We train logistic regression models for this dataset, and for natural model training (with or without ℓ_1 -regularization) we use the Adam optimizer with a learning rate of 0.01, batch size of 32, and 30 training epochs. Adversarial training is similar, except that each example batch is perturbed using the closed-form expression (5).

Spambase. This is another tabular dataset from the UCI Repository, consisting of 4601 instances with 57 numerical attributes (and no categorical ones). The instances are various numerical features of a specific email, and the task is classify the email as spam (label = 1) or not (label = 0). The model and training details are similar to those for the mushroom dataset.

The code for all experiments (included along with the Appendix) was written using Tensorflow 2.0. The following subsections contain results that were left out of the main body of the paper due to space constraints.

I.2. Mushroom Dataset: Average IG-based Feature Impact

We contrast between the weights learned by natural training and adversarial training with $\varepsilon = 0.1$. Since all features in this dataset are categorical, many with cardinalities close to 10, there are too many features in the "exploded" space to allow a clean display, so we instead look at the average Feature Impact (FI, defined in Sec. G) over the (natural, unperturbed) test dataset, see Figure I.4. It is worth noting that several features that have a significant impact on the naturally-trained model have essentially no impact on the adversarially trained model.

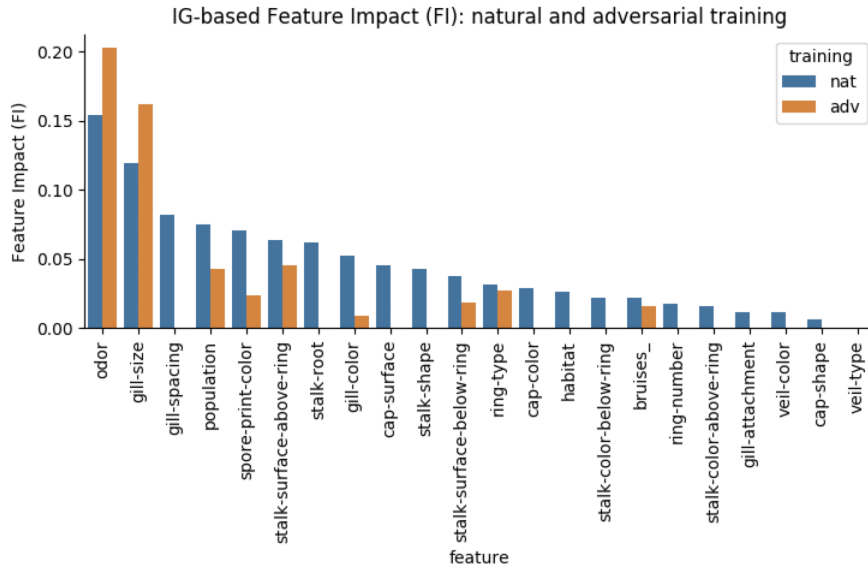


Figure I.4: Comparison of aggregate Feature Impact (FI) for a naturally-trained model, and an adversarially-trained model with $\varepsilon = 0.1$, on the mushroom dataset. The features are arranged left to right in decreasing order of the FI value in the naturally-trained model.

I.3. Spambase: Average IG-based Feature Impact

We fix $\varepsilon = 0.1$ for adversarial training and show in Fig. I.5 a bar-plot comparing the average Feature-Impacts (FI), between naturally-trained and adversarially-trained models. Note how the adversarially trained model has significantly fewer features with non-negligible impacts, compared to a naturally trained model.

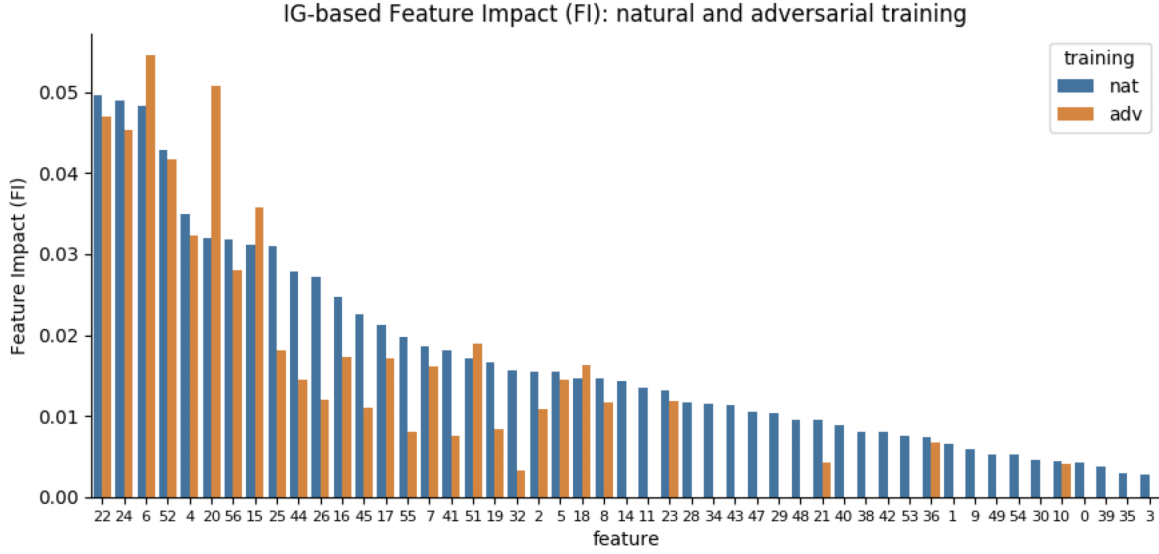


Figure I.5: Comparison of aggregate Feature Impact (FI) for a naturally-trained model, and an adversarially-trained model with $\varepsilon = 0.1$, on the spambase dataset. The features are arranged left to right in decreasing order of their FI in the naturally-trained model. To avoid clutter, we show only features that have an FI at least 5% of the highest FI (across both models).

I.4. MNIST and Fashion-MNIST: examples

Figs. I.6 and I.7 below show IG-based saliency maps of images correctly classified by three model types: Naturally trained un-regularized model, naturally trained model with ℓ_1 -regularization, and an $\ell_\infty(\varepsilon)$ -adversarially trained model. The values of λ and ε are those indicated in Table 1. In each example, all three models predict the correct class with high probability, and we compare the Gini Indices of the IG-vectors (with respect to the predicted probability of the true class). The sparseness of the saliency maps of the adversarially-trained models is visually striking compared to those of the other two models, and this is reflected in the Gini Indices as well.

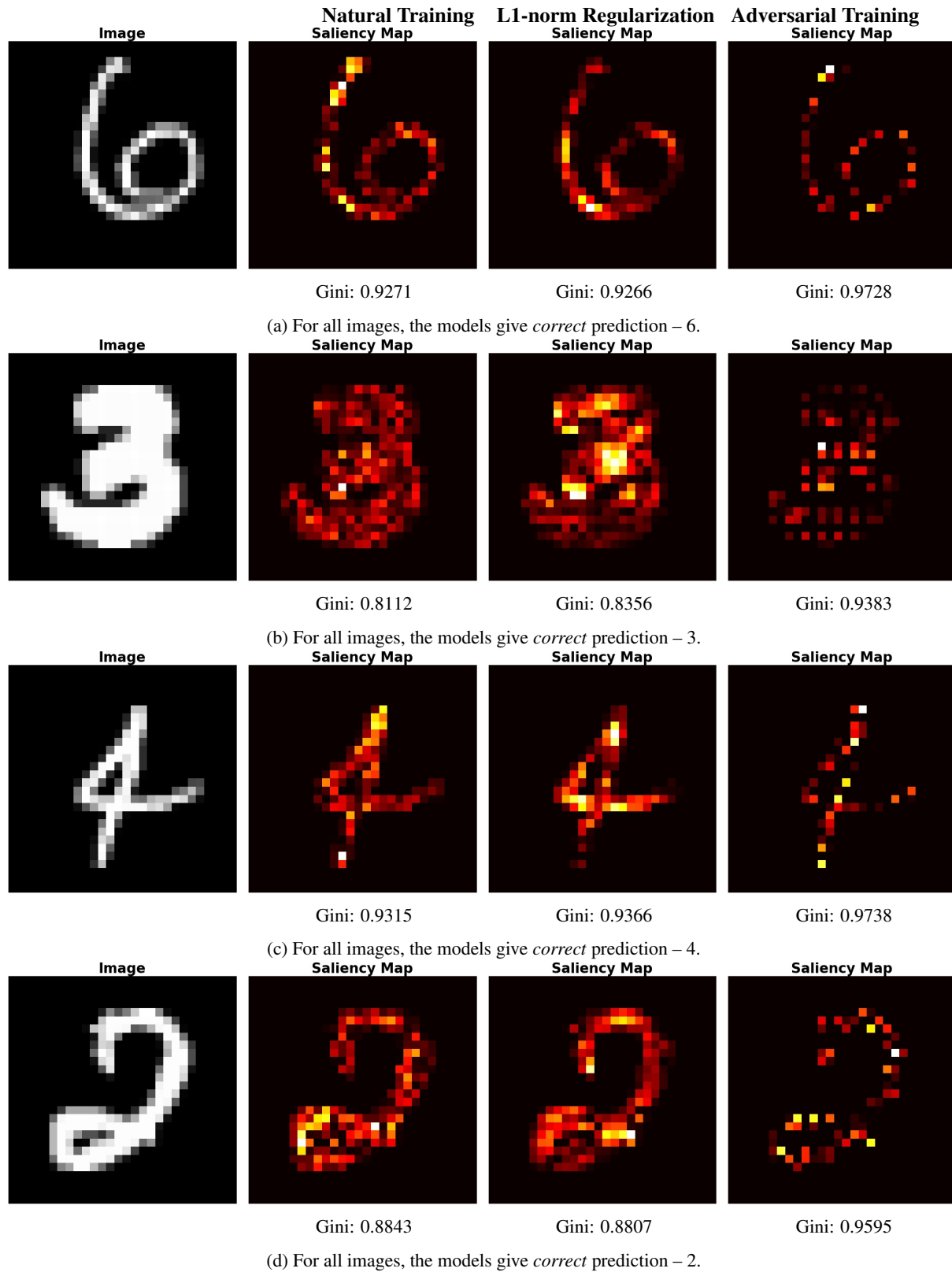


Figure I.6: Some examples on MNIST. We can see the saliency maps (also called feature importance maps), computed via IG, of adversarially trained model are much sparser compared to other models.

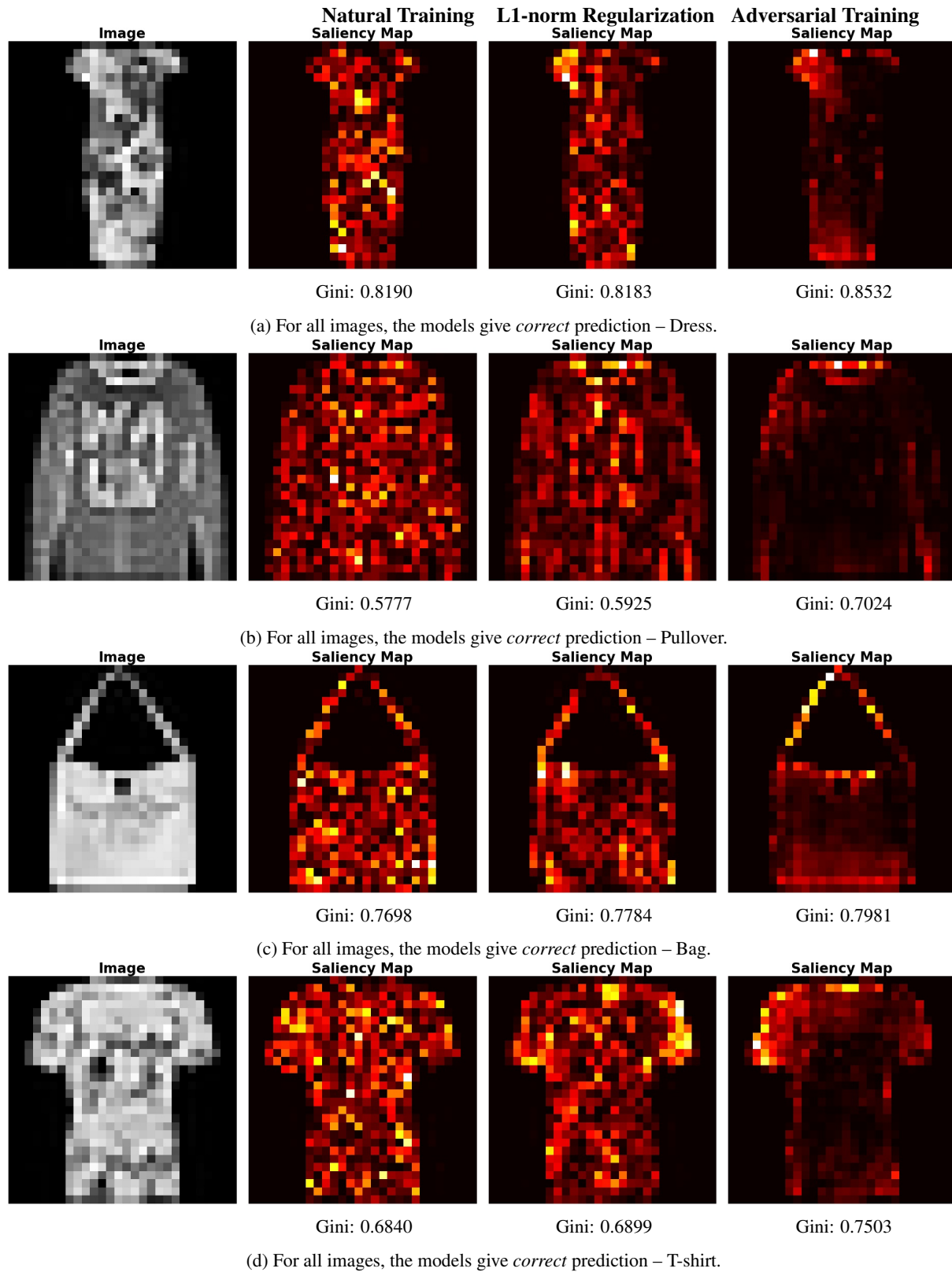


Figure I.7: Some examples on Fashion-MNIST. We can see the saliency maps (also called feature importance maps), computed via IG, of adversarially trained model are much sparser compared to other models.